

Accepted Manuscript

Structure-based virtual screening and optimization of modulators targeting Hsp90-Cdc37 interaction

Lei Wang, Li Li, Zi-Han Zhou, Zheng-Yu Jiang, Qi-Dong You, Xiao-Li Xu



PII: S0223-5234(17)30356-2

DOI: [10.1016/j.ejmech.2017.04.074](https://doi.org/10.1016/j.ejmech.2017.04.074)

Reference: EJMECH 9425

To appear in: *European Journal of Medicinal Chemistry*

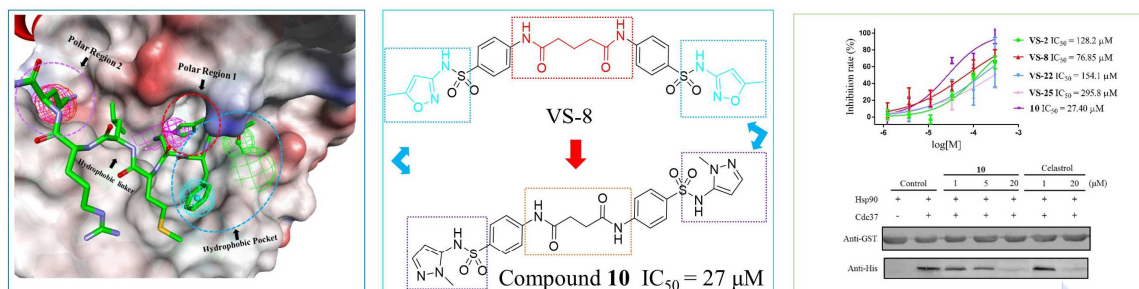
Received Date: 17 February 2017

Revised Date: 26 April 2017

Accepted Date: 29 April 2017

Please cite this article as: L. Wang, L. Li, Z.-H. Zhou, Z.-Y. Jiang, Q.-D. You, X.-L. Xu, Structure-based virtual screening and optimization of modulators targeting Hsp90-Cdc37 interaction, *European Journal of Medicinal Chemistry* (2017), doi: 10.1016/j.ejmech.2017.04.074.

This is a PDF file of an unedited manuscript that has been accepted for publication. As a service to our customers we are providing this early version of the manuscript. The manuscript will undergo copyediting, typesetting, and review of the resulting proof before it is published in its final form. Please note that during the production process errors may be discovered which could affect the content, and all legal disclaimers that apply to the journal pertain.



Virtual Screening

Derivatives Synthesis

Biology

ACCEPTED MANUSCRIPT

Structure-based virtual screening and optimization of modulators targeting Hsp90-Cdc37 interaction

Lei Wang^{a,b}, Li Li^{a,b}, Zi-Han Zhou^c, Zheng-Yu Jiang^{a,b}, Qi-Dong You^{a,b,*} and Xiao-Li Xu^{a,b*}

^aState Key Laboratory of Natural Medicines, and Jiang Su Key Laboratory of Drug Design and Optimization, China Pharmaceutical University, Nanjing 210009, China

^bDepartment of Medicinal Chemistry, School of Pharmacy, China Pharmaceutical University, Nanjing 210009, China

^c Nanjing Foreign Language School, Nanjing 210008, China

* *Corresponding author: Ph.D. Xiao-Li Xu*

Address: China Pharmaceutical University, Nanjing 210009, China.

Tel/Fax: +86 025 83271216.

E-mail address: xuxiao_li@126.com

**Corresponding author: Prof. Qi-Dong You*

Address: China Pharmaceutical University, Nanjing 210009, China.

Tel/Fax: +86 025 83271351.

E-mail address: youqd@163.com

Identification of novel Hsp90 inhibitors to disrupt Hsp90-Cdc37 protein-protein interaction (PPI) could be an alternative strategy to achieve Hsp90 inhibition. In this paper, a series of small molecules targeting Hsp90-Cdc37 complex are addressed and characterized. The molecules' key characters are determined by utilizing a structure-based virtual screening workflow, derivatives synthesis, and biological evaluation. Structural optimization and structure-activity relationship (SAR) analysis were then carried out on the virtual hit of **VS-8** with potent activity, which resulted in the discovery of compound **10** as a more potent regulator of Hsp90-Cdc37 interaction with a promising inhibitory effect ($IC_{50} = 27 \mu M$), a moderate binding capacity ($K_D = 40 \mu M$) and a preferable antiproliferative activity against several cancer lines including MCF-7, SKBR3 and A549 cell lines ($IC_{50} = 26 \mu M$, $15 \mu M$ and $38 \mu M$ respectively). All the data suggest that compound **10** exhibits moderate inhibitory effect on Hsp90-Cdc37 and could be regard as a first evidence of a non-natural compound targeting Hsp90-Cdc37 PPI.

Heat shock protein 90 (Hsp90) has been recognized as a crucial role for cell cycle control, protein assembly, kinase folding, cell survival and many signaling pathways [1-3]. Targeting Hsp90 to inhibit its biological function is a therapeutic strategy to treat cancer, and to date, over 20 distinct N-terminal Hsp90 inhibitors have entered into clinical trials [4]. These inhibitors are composed of geldanamycin (GA) analogues, resorcinol analogues, purine analogues and other synthetic inhibitors that all of them target the Hsp90 ATP pocket [5]. However, several severe side-effects have been reported in some clinical trials and none of them have been approved by the Food and Drug Administration (FDA) [6-8]. ATP-competitive inhibitors could induce heat shock responses by upregulating the multifarious stress inducible heat shock proteins, such as Hsp70, which is inevitable and ultimately contribute the insensitivity and resistance of Hsp90 inhibitors on tumor cells [8]. The Hsp90 chaperone machine works through a multi-cycle process [9]. Simply inhibiting the ATP hydrolysis of Hsp90 will inevitably impair some regular client proteins including tyrosine kinases, signal transduction proteins, cell-cycle regulatory proteins, anti-apoptotic proteins and telomerases [2]. The toxicity and heat shock response induced by Hsp90 ATPase inhibitors are possibly because of the partial damage of those proteins.

During the maturation of client proteins of Hsp90, ATP hydrolysis is only one step of this complicated procedures. Multiple co-chaperones, such as Hsp70, Hsp40, HOP, Cdc37, and Aha1, are indispensable of each other [10, 11]. Protein kinases are a significant part of Hsp90 chaperone client proteins and play crucial roles in the occurrence and development of tumor growth [12]. Among them, more than 50% of the client proteins need the co-chaperone Cdc37 to regulate their correct folding, transformation and maturation [13]. Cdc37, known as protein kinases-specific Hsp90 co-chaperone, plays an essential role in

loading protein kinases to Hsp90 chaperone machine, leading to natural maturation [14]. In addition to classic ATP-competitive Hsp90 inhibitors, disrupting Hsp90-Cdc37 PPI will affect certain protein kinases rather than all the client proteins of Hsp90 which definitely exhibit higher specificity and lower potential toxicity and avoid the side effects and [15]. This is as an alternative and promising strategy to break through the barriers of classic Hsp90 ATPase inhibitors currently in clinical trials.

At present the rational development of Hsp90-Cdc37 have been challenging due to the complexity of protein-protein interaction. Hsp90-Cdc37 PPI have been reported all exhibited a low micromolar binding ability *in vitro* [16, 17]. Nevertheless, the X-ray crystal structure and NMR spectroscopy of the mid-domain of Cdc37 and N-terminal of Hsp90 were presented in 2004 and 2009 respectively, providing a great foundation for development of small molecular inhibitors to disrupt Hsp90-Cdc37 PPI [17-19]. In 2008, one of the potent ingredients from the extracts of Celastraceae plants, Celastrol, was reported to exhibit potency of Hsp90-Cdc37 disruption by binding to a charged pocket of Hsp90 N-terminal [20]. However, another result they put forward in 2009 demonstrated that celastrol prevented Hsp90 C-terminal from trypsin digestion by a direct binding mechanism through a fingerprinting assay [21]. Thus, celastrol might reveal its potency by multiple regulation mechanisms. Compared to celastrol, other reported modulators including withaferin A (WA) [22], FW-04-806 [23], apigenin [24], sulforaphane [25] and kongensin A (KA) showed similar low activities. As shown in Fig. 1, all of these modulators are natural products showing the absence of target specificity, certainty in modulation mechanism, specific binding site and co-crystal structures, leading to no ideal lead compounds for future modification and development. Thus, small molecules targeting the Hsp90-Cdc37 PPI interface with high affinity and specificity are urgently required.

The most common method to obtain PPI modulators is initiated from the peptides directly derived from the PPI binding interface [26]. According to our previous study [27], we utilized the potential peptides derived from Cdc37 to explore the detailed binding site of Hsp90-Cdc37 for the discovery of small molecules. In this paper, we report our workflow of discovery and identification of small molecules targeting Hsp90-Cdc37 PPI by a virtual screening-based method combined with biological validation. Five hundred thousand compounds in Specs and NCI databases were screened by pharmacophore and cross-docking filtrations. Thirty-one compounds were obtained and purchased for further identification in *in vitro* assays. Finally, **VS-8** (specs ID: AN-329/40718894) revealed weak activity *in vitro* (IC_{50} values: 77 μ M) and exhibited anti-proliferative potency against several cancer lines including MCF-7, SKBR3 and A549 cell lines. To enhance the potency and explore the structure relationship of **VS-8**, 16 derivatives were designed and synthesized to reveal compound **10**, which exhibited more promising inhibitory effect ($IC_{50} = 27 \mu$ M), better binding capacity ($K_d = 40 \mu$ M) and preferable antiproliferative activity against MCF-7, SKBR3 and A549 cell lines ($IC_{50} = 26 \mu$ M, 15 μ M and 38 μ M respectively) compared to **VS-8**. All the data suggest that compound **10** exhibited moderate inhibitory effect on Hsp90-Cdc37 and could be regard as a first evidence of a non-natural compound targeting Hsp90-Cdc37 PPI.

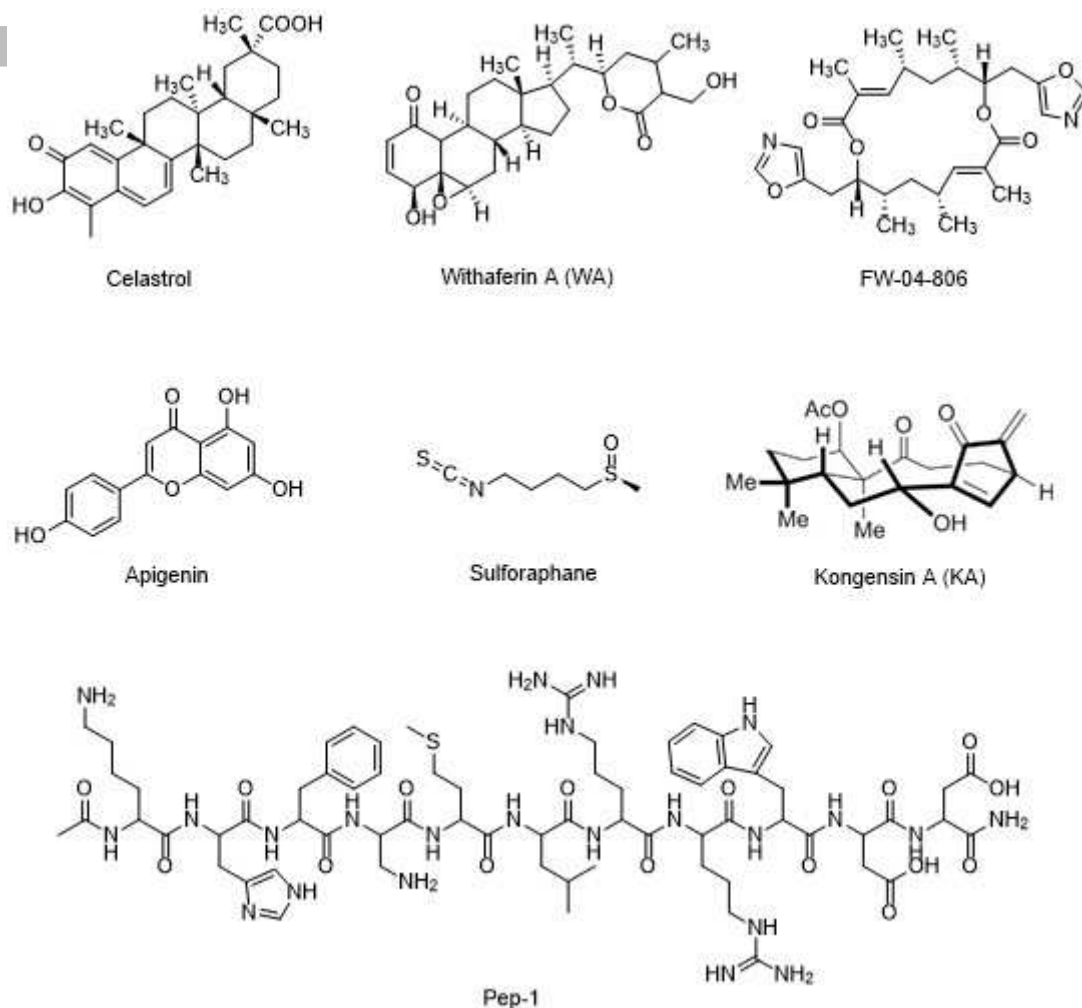


Figure 1. 2D structures of the reported modulators targeting Hsp90-Cdc37 PPI.

2. Materials and Methods

2.1 Compounds and Reagents

Positive compounds including celastrol (Selleck, TX, USA), GA-FITC (BML-E1361, Enzo Life Sciences, USA, FITC labelled geldanamycin, used as a probe molecule in fluorescence polarization competitive assay) and 17-DMAG (Selleck, TX, USA) were dissolved in DMSO (sigma, St. Louis, MO, USA) and stored at $-20\text{ }^{\circ}\text{C}$ in a final concentration of 10 mM before use.

2.2 Computational methods

2.2.1 Pharmacophore generation

The basic pharmacophore model was generated from the crystal structure of

Hsp90-Cdc37 (PDB: 1US7). To obtain detailed information of the ligand-receptor binding mode, a Cdc37 derived peptides docking model was utilized to construct the final pharmacophore [27]. Receptor-Ligand Pharmacophore Generation protocol in Accelrys Discovery Studio (DS) 3.0 (Accelrys Inc., San Diego, CA, USA) was utilized to construct the pharmacophore model. Finally, based on hot-spots and binding mode analysis, we manually selected the indispensable pharmacophore elements that contain two hydrogen bond donors (HBD), one hydrogen bond acceptor (HBA), one hydrophobic feature and one positive ionizable center.

2.2.2 Pharmacophore and docking screening

The chemical databases (Specs and NCI database) with 500,000 molecules were screened using the ensemble pharmacophore model by ligand pharmacophore mapping module in DS 3.0. Considering the complexity of the pharmacophore model and harsh criteria for eligible ligands, one feature can be omitted in the ligand-pharmacophore mapping procedure. All the molecules which fitted at least four pharmacophores (1532 remained) were aligned in DS 3.0 and processed the cross-docking procedure. These ligands were docked into Hsp90 protein structure by Libdock, Flexdock, CDOCKER and Glod5.0 (DS 3.0). The root-mean-square deviation (RMSD) was utilized to compare the differences between the docked poses and co-crystallized pose to measure docking reality. Finally, 31 compounds with preferable docking scores and binding models were picked out for purchasing list and further biological validation.

2.3 Chemistry

All reagents in this paper were purchased from commercial sources. Rotary evaporator (BüchiRotavapor) below 50 °C under reduced pressure was used to concentrate all organic solutions. Melting points were determined using a Melt-Temp II apparatus. Bruker AV-300

instrument was utilized to measure all ^1H NMR spectra. Deuterated solvents were used to dissolve all compounds with tetramethylsilane (TMS) as internal standard. Shimadzu GCMS-2010 instruments were used to obtain EI-MS and Water Q-Tofmicro mass spectrometer was used to obtain ESI-mass and high resolution mass spectra (HRMS). HPLC was performed on Agilent C18 column (4.6 mm \times 150 mm, 3.5 μm) to determine the purity of all compounds.

2.3.1 General procedure for preparation of 2a-e.

Malonyl chloride (2a). Malonic acid (1.4 g, 10 mmol) was directly dissolved in thionyl chloride (10 mL) and then heated to reflux for 2 h. The excess thionyl chloride was removed by rotary evaporator below 50 $^\circ\text{C}$ under reduced pressure. The crude product was obtained and directly used in the next step. **2b-2e** were obtain using the similar procedures of **2a**

2.3.2 General method for the preparation of 5f-5o.

4-amino-N-(5-methylisoxazol-3-yl)benzenesulfonamide (5f).
3-amino-5-methylisoxazole (1.18 g, 12 mmol) was added to the solution of THF (20 mL) and pyridine (1 mL). The reaction mixture was stirred at room temperature for 6 h after 4-acetamidobenzenesulfonyl chloride (2.34 g, 10 mmol) was added to the reaction solution. After the completion of the reaction monitored by TLC, the solvent was remove. Then, 30 mL of 0.5 M hydrochloric acid was added and a lot of precipitation was precipitated for filtration. The crude solid was washed with water and directly used in the next step. All the intermediates were dissolved in 20% NaOH solution and the reaction mixtures were heated to reflux in an oil bath for 2 h. Then the reaction solution was quenched with 2 M hydrochloric acid to pH 7.4, resulting a lot of white solid. The crude product was obtained and washed with 5*10 mL water, then dried overnight in a vacuum desiccator, yielding **5f** as a white solid, yield 86%; mp 168-172 $^\circ\text{C}$. ^1H NMR (300 MHz, DMSO, δ) 7.55 (d, 2H, $J =$

7.08 Hz), 6.78-6.82 (d, 2H, $J = 8.56$ Hz), 6.35 (s, 1H), 6.05 (s, 2H), 2.36 (s, 3H). HRMS (ESI): found 239.2656 ($C_{10}H_{10}N_2O_3S$, $[M + H]^+$, requires 239.2641). HPLC (80:20 methanol:water with 1% TFA): $t_R = 3.86$ min, 98.1%.

5g to **5o** were obtained using the similar procedures of **5f**.

2.3.2 General synthesis procedure of 1-16.

N1,N3-bis(4-(N-(5-methylisoxazol-3-yl)sulfamoyl)phenyl)malonamide (**1**). **5f** (253 mg, 1 mmol) was dissolved in the solution of THF (10 mL) and pyridine (1 mL) before **2a** (240 mg, 2 mmol) was dropwise added. Then the reaction mixture was stirred at room temperature overnight until the white solid was precipitated. The crude product was filtered and recrystallized with ethanol to give a **1** as a light-yellow solid, yield 72%; mp 213-216 °C, 1H NMR (300 MHz, DMSO, δ) 10.58 (s, 2H), 7.79 (d, 8H, $J = 3.01$ Hz), 6.10 (s, 2H), 3.55 (s, 2H), 2.28 (s, 6H). HRMS (ESI): found 573.0863 ($C_{23}H_{22}N_6O_8S_2$, $[M-H]^-$, requires 573.0868). HPLC (80:20 methanol:water with 1% TFA): $t_R = 4.64$ min, 96.91%.

N1,N4-bis(4-(N-(5-methylisoxazol-3-yl)sulfamoyl)phenyl)succinamide (**2**). The same procedure as **1**, white solid, yield 83%; mp 263-265 °C, 1H NMR (300 MHz, DMSO, δ) 11.30 (s, 2H), 10.46 (s, 2H), 7.79 (s, 8H), 6.13 (s, 2H), 2.72 (s, 4H), 2.31 (s, 6H). HRMS (ESI): found 611.0262 ($C_{24}H_{24}N_6O_8S_2$, $[M+Na]^+$, requires 611.0091). HPLC (80:20 methanol:water with 1% TFA): $t_R = 4.12$ min, 99.91%.

N1,N6-bis(4-(N-(5-methylisoxazol-3-yl)sulfamoyl)phenyl)adipamide (**3**). The same procedure as **1**, white solid, yield 89%; mp 266-267 °C, 1H NMR (300 MHz, DMSO, δ) 11.31 (s, 2H), 10.32 (s, 2H), 7.76 (s, 8H), 6.11 (s, 2H), 2.36 (s, 4H), 2.28 (s, 6H), 1.61 (s, 4H). HRMS (ESI): found 639.1452 ($C_{26}H_{28}N_6O_8S_2$, $[M+Na]^+$, requires 625.1426). HPLC (80:20 methanol:water with 1% TFA): $t_R = 4.25$ min, 98.95%.

N1,N4-bis(4-(N-(5-methylisoxazol-3-yl)sulfamoyl)phenyl)terephthalamide (**4**). The

same procedure as **1**, yellow solid, yield 65%; mp 223-225 °C, ¹H NMR (300 MHz, DMSO, δ) 11.31 (s, 2H), 10.59 (s, 2H), 8.34 (s, 2H), 7.82-7.67 (m, 8H), 7.37 (d, 2H, *J* = 6.04Hz) 6.12 (s, 2H), 2.29 (s, 6H). HRMS (ESI): found 659.6504 (C₂₈H₂₄N₆O₈S₂, [M+Na]⁺, requires 659.6511). HPLC (80:20 methanol:water with 1% TFA): t_R = 4.21 min, 98.25%.

N1,N3-bis(4-(N-(4,5-dimethylisoxazol-3-yl)sulfamoyl)phenyl)malonamide (**5**). The same procedure as **1**, light yellow solid, yield 64%; mp 230-234 °C, ¹H NMR (300 MHz, DMSO, δ) 10.94 (s, 2H), 10.64 (s, 2H), 7.79 (d, 4H, *J* = 8.86Hz), 7.71 (d, 4H, *J* = 8.82Hz), 3.58 (s, 2H), 2.08 (s, 12H). HRMS (ESI): found 625.6431 (C₂₅H₂₆N₆O₈S₂, [M+Na]⁺, requires 625.6423). HPLC (80:20 methanol:water with 1% TFA): t_R = 4.18 min, 99.82%.

N1,N3-bis(4-(N-(1-methyl-1H-pyrazol-5-yl)sulfamoyl)phenyl)malonamide (**6**). The same procedure as **1**, white solid, yield 75%; mp 277-279 °C, ¹H NMR (300 MHz, DMSO, δ) 10.86 (s, 2H), 7.82 (d, 4H, *J* = 8.71Hz), 7.67 (d, 4H, *J* = 9.01Hz), 7.26 (d, 2H, *J* = 1.82Hz), 5.60 (d, 2H, *J* = 1.84Hz), 3.61 (s, 2H), 3.56 (s, 6H). HRMS (ESI): found 595.1326 (C₂₃H₂₄N₈O₆S₂, [M+Na]⁺, requires 595.1321). HPLC (80:20 methanol:water with 1% TFA): t_R = 3.98 min, 99.91%.

N1,N3-bis(4-(N-phenylsulfamoyl)phenyl)malonamide (**7**). The same procedure as **1**, white solid, yield 89%; mp 202-204 °C, ¹H NMR (300 MHz, DMSO, δ) 10.54 (s, 2H), 7.69 (s, 8H), 7.21-7.18 (m, 4H), 7.07-7.04 (m, 4H), 7.00 (s, 2H), 3.50 (s, 2H). HRMS (ESI): found 587.1136 (C₂₇H₂₄N₄O₈S₂, [M+Na]⁺, requires 587.1129). HPLC (80:20 methanol:water with 1% TFA): t_R = 4.66 min, 99.85%.

N1,N4-bis(4-(N-(4,5-dimethylisoxazol-3-yl)sulfamoyl)phenyl)succinamide (**8**). The same procedure as **1**, white solid, yield 92%; mp 247-249 °C, ¹H NMR (300 MHz, DMSO, δ) 10.91 (s, 2H) 10.48 (s, 2H), 7.78 (d, 4H, *J* = 8.98Hz), 7.68 (d, 4H, *J* = 8.91Hz) 2.72 (s, 4H), 2.07 (s, 6H), 1.61 (s, 6H). HRMS (ESI): found 639.1303 (C₂₆H₂₄N₆O₆S₂, [M+Na]⁺, requires

639.1302). HPLC (80:20 methanol:water with 1% TFA): $t_R = 4.22$ min, 99.14%.

N1,N4-bis(4-(N-(thiazol-2-yl)sulfamoyl)phenyl)succinamide (**9**). The same procedure as **1**, pink solid, yield 86%; mp > 300 °C, $^1\text{H NMR}$ (300 MHz, DMSO, δ) 12.59 (s, 2H), 10.27 (s, 2H), 7.62 (s, 8H), 7.14 (d, 2H, $J = 4.62\text{Hz}$), 6.71 (d, 2H, $J = 4.62\text{Hz}$), 2.41-2.39 (m, 4H). HRMS (ESI): found 615.6814 ($\text{C}_{22}\text{H}_{20}\text{N}_6\text{O}_6\text{S}_4$, $[\text{M}+\text{Na}]^+$, requires 615.6810). HPLC (80:20 methanol:water with 1% TFA): $t_R = 3.82$ min, 99.85%.

N1,N4-bis(4-(N-(1-methyl-1H-pyrazol-5-yl)sulfamoyl)phenyl)succinamide (**10**). The same procedure as **1**, white solid, yield 88%; mp > 300 °C, $^1\text{H NMR}$ (300 MHz, DMSO, δ) 10.48 (s, 2H), 10.18 (s, 2H), 7.80 (d, 4H, $J = 8.40\text{Hz}$), 7.66 (d, 4H, $J = 8.76\text{Hz}$), 7.28 (d, 2H, $J = 1.65\text{Hz}$), 5.62 (d, 2H, $J = 4.08\text{Hz}$), 3.58 (d, 6H, $J = 4.62\text{Hz}$), 2.74 (s, 4H). HRMS (ESI): found 609.6428 ($\text{C}_{24}\text{H}_{26}\text{N}_8\text{O}_6\text{S}_2$, $[\text{M}+\text{Na}]^+$, requires 609.6419). HPLC (80:20 methanol:water with 1% TFA): $t_R = 4.72$ min, 99.67%.

N1,N4-bis(4-(N-phenylsulfamoyl)phenyl)succinamide (**11**). The same procedure as **1**, white solid, yield 88%; mp 280-281 °C, $^1\text{H NMR}$ (300 MHz, DMSO, δ) 10.29 (s, 2H), 10.05 (s, 2H), 7.58 (s, 8H), 7.11 (s, 5H), 6.97 (s, 5H), 2.56 (s, 2H), 2.41 (s, 2H). HRMS (ESI): found 601.1205 ($\text{C}_{28}\text{H}_{26}\text{N}_4\text{O}_6\text{S}_2$, $[\text{M}+\text{Na}]^+$, requires 601.1186). HPLC (80:20 methanol:water with 1% TFA): $t_R = 3.95$ min, 99.96%.

N1,N4-bis(4-(N-(pyridin-2-yl)sulfamoyl)phenyl)succinamide (**12**). The same procedure as **1**, light yellow solid, yield 88%; mp 280-281 °C, $^1\text{H NMR}$ (300 MHz, DMSO, δ) 10.35 (s, 2H), 8.00 (d, 2H, $J = 6.84\text{Hz}$), 7.78 (d, 4H, $J = 8.88\text{Hz}$), 7.70-7.65 (m, 6H), 7.10 (d, 2H, $J = 8.58\text{Hz}$), 6.87-6.83 (m, 2H), 2.66 (s, 4H). HRMS (ESI): found 603.1112 ($\text{C}_{26}\text{H}_{24}\text{N}_6\text{O}_6\text{S}_2$, $[\text{M}+\text{Na}]^+$, requires 603.1091). HPLC (80:20 methanol:water with 1% TFA): $t_R = 4.08$ min, 99.63%.

N1,N4-bis(4-(N-(4-methylpyrimidin-2-yl)sulfamoyl)phenyl)succinamide (**13**). The

same procedure as **1**, white solid, yield 81%; mp 254-255 °C, ¹H NMR (300 MHz, DMSO, δ) 11.49 (s, 2H), 10.30 (s, 2H), 8.21 (d, 2H, *J* = 5.10Hz), 7.80 (d, 2H, *J* = 8.85Hz), 7.63 (d, 2H, *J* = 8.85Hz) 6.80-6.77 (m, 2H), 2.41-2.40 (m, 4H), 2.20 (s, 6H). HRMS (ESI): found 633.6648 (C₂₆H₂₆N₈O₆S₂, [M+Na]⁺, requires 633.6639). HPLC (80:20 methanol:water with 1% TFA): t_R= 3.82 min, 96.19%.

N1,N4-bis(4-(N-(pyrimidin-2-yl)sulfamoyl)phenyl)succinamide (**14**). The same procedure as **1**, white solid, yield 81%; mp 254-255 °C, ¹H NMR (300 MHz, DMSO, δ) 11.58 (s, 2H), 10.31 (s, 2H), 8.61 (d, 4H, *J* = 8.85Hz), 7.80 (d, 4H, *J* = 8.85Hz), 7.57-7.50 (m, 4H), 6.95-6.92 (m, 2H), 2.40 (s, 4H). HRMS (ESI): found 605.6122 (C₂₄H₂₂N₈O₆S₂, [M+Na]⁺, requires 605.6127). HPLC (80:20 methanol:water with 1% TFA): t_R= 4.10 min, 99.92%.

N1,N4-bis(4-(N-(6-methoxypyridazin-3-yl)sulfamoyl)phenyl)succinamide (**15**). The same procedure as **1**, white solid, yield 78%; mp 270-271 °C, ¹H NMR (300 MHz, DMSO, δ) 10.26 (s, 2H), 7.87-7.60 (m, 10H), 7.24 (d, 2H, *J* = 9.63Hz), 3.74 (s, 6H), 2.59 (s, 4H). HRMS (ESI): found 665.1214 (C₂₆H₂₆N₈O₈S₂, [M+Na]⁺, requires 665.1207). HPLC (80:20 methanol:water with 1% TFA): t_R= 3.81 min, 99.89%.

N1,N4-bis(4-((2-(diaminomethylene)hydrazinyl)sulfonyl)phenyl)succinamide (**16**). The same procedure as **1**, yellow solid, yield 65%; mp 251-253 °C, ¹H NMR (300 MHz, DMSO, δ) 8.79 (t, 1H, *J* = 1.44Hz), 7.88-7.83 (m, 1H), 7.36-7.31 (m, 3H), 6.61-6.51 (m, 8H), 2.41 (t, 4H, *J* = 1.77Hz). HRMS (ESI): found 563.5724 (C₁₈H₂₄N₁₀O₆S₂, [M+Na]⁺, requires 563.5729). HPLC (80:20 methanol:water with 1% TFA): t_R= 4.10 min, 96.32%.

2.4 Biology

2.4.1 Expression and purification of Hsp90 and Cdc37.

The protein expression and purification assays were carried out as previously described [27].

2.4.2 Homogeneous Time-Resolved Fluorescence (HTRF) assay

For each HTRF assay, 4 μL of His-tagged full-length Hsp90 and 4 μL of GST-tagged Cdc37 M were mixed into 384-well black low volume plate (Greiner#784076) in PBS buffer (containing additional 400 mM KF, pH=7.4) with a final concentration of 250 nM, respectively. Subsequently, 4 μL of a different gradient of diluted compounds (ranging from 300 μM to 1.23 μM with three times dilution) were added into the plate for 1 h incubation at 37 °C. Another 0.5 h incubation at 37 °C was performed after adding 4 μL of anti-GST-Cryptate (61GSTKLA, CISBIO) and 4 μL of anti-6His-XL665 (61HISXLA, CISBIO) detection reagent to reach a final 20 μL testing system. Molecular Device (SpectraMax paradigm; $\lambda_{\text{ex}} = 320 \text{ nm}$, $\lambda_{\text{em}} = 665 \text{ nm}$ and 620 nm) was carried out to measure the time-resolved fluorescence values. The final HTRF ratio was obtained by a two-wavelength signal proportion calculated as following equation: (Signal 665 nm/Signal 620 nm) $\times 10000$. Negative control (without addition of compounds) and blank control (detection reagent only) were performed for each test. All data were analyzed by GraphPad Prism 5.0 software.

2.4.3 ATPase inhibition assay

Hsp90 ATPase inhibition assay was performed using Discover RX ADP Hunter™ Plus Assay Kit (Discovery, Fremont, CA). Following the instructions, constant concentration of compounds (diluted to a final concentration of 100 μM with buffer containing 15 mM HEPES, 20 mM NaCl, 1 mM EDTA, 10 mM MgCl_2 and 0.02% Tween20, pH = 7.4) and positive control (celastrol and 17-DMAG) were tested in 384-well black plates at 37 °C. Each well was filled with 20 μL diluted compound, 20 μL Hsp90 protein (5 μM) and 20 μL

ATP (100 μ M) for 1 h incubation. 10 μ L detection reagent A and 20 μ L detection reagent B was added subsequently and incubated at room temperature for 30 mins before final determination. To examine the ADP generation, a Varioskan multimode microplate spectrophotometer (Thermo Scientific Varioskan Flash, 540 nm excitation and 620 nm emission) was used. Background values were measured in a condition without protein and ligands, while negative control was determined in a solution without ligand and was regarded as 100% protein activity.

2.4.4 Fluorescence polarization (FP) competitive assay

Generally, the FP experiments was performed as previously reported [28]. The FP experiments were carried out using the excitation and emission filters. 20 μ L Hsp90 protein and 20 μ L GA-FITC probe mixture (100 mM Tris at pH 7.4, 20 mM KCl, 6 mM MgCl₂, 5 mg/ml BSA, 100 nM Hsp90, 10 nM GA-FITC) were added to 384-well black plates combined with 20 μ L diluted compounds (constant concentration: 100 μ M). After 30 min incubation at room temperature in the dark, fluorescence polarization values were measured on a SpectraMax multimode microplate reader (Molecular Devices SpectraMax Paradigm; Excitation wavelength 485 nm, Emission wavelength 535 nm). The final inhibition ratio was calculated using GraphPad Prism 5.0. The inhibition of the inhibitors were determined by equation $\% \text{inhibition} = 1 - (P_{\text{obs}} - P_{\text{min}}) / (P_{\text{max}} - P_{\text{min}})$. P_{max} refers to the polarization values of the wells containing protein Hsp90 and the GA-FITC probe. P_{min} refers to the polarization values of free GA-FITC probe and P_{obs} refers to the wells simply containing the inhibitors of a certain concentration under the assay conditions.

2.4.5 Biolayer interferometry (BLI) assay

General experiment procedures were described previously [29]. The binding capacity between the compounds and the Hsp90 protein was determined by biolayer interferometry

using an Octet Red 96 instrument (ForteBio Inc.). All the assays were performed on Corning 96-well black plate and data were collected at 25 °C. Before the protein was immobilized onto the Aminopropylsilane (APS, ForteBio Inc., Menlo Park, CA) biosensors, all the tips were placed in the buffer of 0.1 M PBS to establish a pre-baseline. Next, the experiments were composed of following steps: (1) baseline 1, sensors transferred to the 0.1 M PBS buffer for 120 s equilibration; (2) loading, sensor tips were moved to Hsp90 protein wells for 600 s immobilization; (3) baseline 2, sensors were moved to plates containing 0.1 M PBST for another 120 s equilibration; (4) association, sensors moved to ligand buffer for 300 s to measure K_{on} ; (5) dissociation, sensors moved to 0.1 M PBST buffer for 300 s to measure K_{off} . Four concentrations of each compound were utilized to obtain the final curve (ranging from 100 μ M to 12.5 μ M). All the data were analyzed by ForteBio data analysis software and the equilibrium dissociation constant (K_D) values were calculated using the equation ($K_D = K_{off}/K_{on}$).

2.4.6 GST pull-down assay

GST pull-down experiments were conducted using Pierce™ GST Protein Interaction Pull-Down Kit (Thermo Scientific). Loading buffer consisted of 25 mM Tris, 0.15 M NaCl (pH 7.2) and elution buffer contained an extra 10 mM reduced glutathione. 10 μ g purified GST-Hsp90N protein (N-terminal Hsp90 with GST-tag) was used as bait protein to immobilize on the sepharose-contained resin in the Pierce Spin Columns for binding to the substrates. Compounds and celastrol were added into the columns after incubation with Cdc37 for 1 h at 37 °C. In addition, then centrifugation (1 min at 1,000 \times g, 4 °C) was performed to remove solution containing Cdc37 (prey protein) before elution buffer was added. The columns were washed by loading buffer three times and the eluent was collected via centrifugation (1 min at 1,000 \times g, 4 °C) for analysis of the eluted protein by SDS-PAGE

2.4.7 Cell culture

The human cancer cell lines MCF-7, SKBR-3 and A549 were purchased from American Type Culture Collection (ATCC) or Cell Culture Center at the Institute of Basic Medical Sciences, Chinese Academy of Medical Sciences. MCF-7 cells were cultured in MEM, SKBR-3 cells were cultured in RPMI-1640 medium and A549 cells were cultured in F12K. All of them were supplemented with 10% fetal calf serum and antibiotics. Cells were maintained in a 37 °C incubator (Thermo, USA) with 95% humidity and 5% CO₂.

2.4.8 Western Blot Analysis

The expression levels of client proteins were determined by Western blot assay. SKBR-3 cells were treated with multiple diluted compound **10** (1 μM, 10 μM and 50 μM) for 24 h. Celastrol (1 μM and 10 μM) was chosen as the reference. Lysis buffer (50 mM Tris-HCl, pH 7.5, 150 mM NaCl, 1 mM EDTA, 1% NP-40, 0.2 mM PMSF, 0.1 mM NaF and 1.0 mM DTT) was used to lyse the cells after they were rinsed with PBS and trypsinized. Then, the lysates were centrifuged at 12000 rpm for 10 min at 4 °C and the supernatants were collected. The concentration of the protein was determined by BCA assay (Thermo, Waltham, MA). Equal amounts of the total protein extracts were determined by SDS-PAGE. The primary antibodies were anti-Hsp90 (#4874, Cell Signaling Technology, Inc., USA), anti-Akt (#9272, Cell Signaling Technology, Inc., USA), anti-Cdk4 (#12790, Cell Signaling Technology, Inc., USA) and anti-β-actin (#66009-1-Ig, Proteintech Group, Inc., China). Subsequently, the membranes were treated with a DyLight 800-labeled secondary antibody (#072-07-15-06, KPL, USA) at 37 °C for 1 h. Finally, the Odyssey infrared imaging system (LI-COR, Lincoln, Nebraska, USA) were used for scanning.

2.4.9 Anti-proliferative assay

Cell-based MTT assay was utilized to evaluate the anti-proliferative activity in MCF-7, SKBR-3 and A549 cells. All the Cells were seeded in 96-well plates (10000/well) and maintained for 24 h. Next, the compounds dissolved in DMSO in disparate concentrations was added, and cells were incubated for 72 h. Additional incubation in 37 °C was conducted after adding 20 μ L MTT solution (5 mg/mL in PBS). Next, 150 μ L DMSO was added in the wells to dissolve the MTT-formazan crystal, which generated only in viable cells. The OD values were determined by the Elx800 absorbance microplate reader (BioTek, Vermont, USA) at 490 nm. According to the linear relationship between OD values and the number of viable cells, the IC₅₀ value was calculated from parallel experiments via Graphpad Prim 6.0 software and performed as the mean \pm SD.

3. Results and Discussion

3.1 Pharmacophore model generation

Since numerous protein crystal structures have been determined, the receptor-ligand complex based pharmacophore method turns to be more and more significant and efficient [30]. To discover non-peptide modulators targeting Hsp90-Cdc37 PPI, the significant chemical features in binding hot-spots were generated to perform multiple pharmacophore elements based on the binding mode of active peptides and complex crystal structure [29]. As shown in Fig. 2, two polar regions are composed of a histidine and a terminal arginine which have been demonstrated to be the determinants for the recognition and binding between target and ligands. Phenylalanine and the terminal acetyl represent a hydrophobic pocket which contribute to the main entropy for binding. The hydrophobic linker (providing less binding contribution) occupies a superficial cavity on Hsp90 and exhibits a moderate distance of approximately 15 Å. In addition, it has been reported that the side-chain of

Arg167 in Cdc37 forms an electrostatic interaction and a H-bond with the side-chain of Glu47 in Hsp90, which were regarded as the most decisive factor for Hsp90-Cdc37 PPI in the crystal structure [17]. Thus, one positive feature at polar region 2 is indispensable for ligand binding. All these results taken together resulted in five pharmacophore features: three H-bond features, one hydrophobic feature and one ionizable feature.

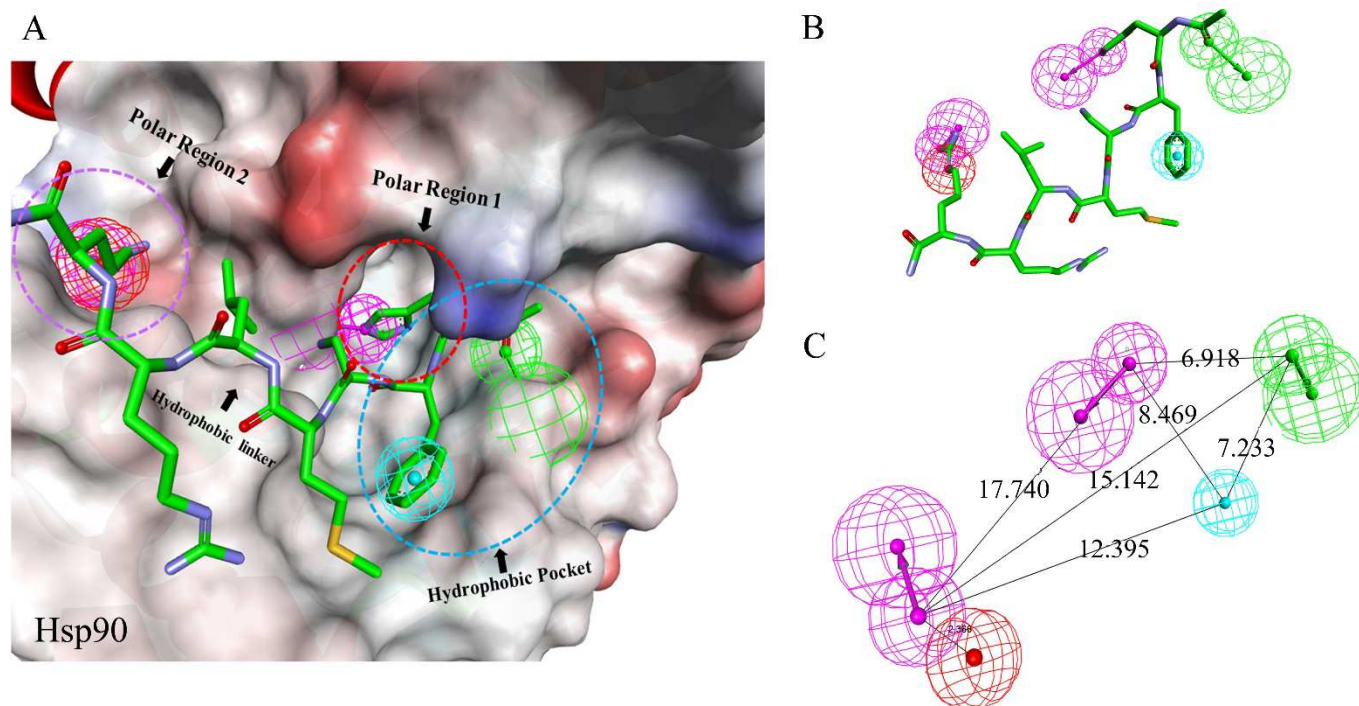


Figure 2. Pharmacophore model generation based on active peptide which is represented in green sticks. The surfaces represent Hsp90. (A) Ligand and receptor-based pharmacophore generation containing two polar regions and one hydrophobic pocket. (B) The final pharmacophore used for screening. Pharmacophore features are described as follows: hydrogen bond donor (HBD), violet; hydrogen bond acceptor (HBA), green; hydrophobic center, azure; positive ionizable center, red. (C) Pharmacophore distance. The distance between certain features is represented in Å.

3.2 Pharmacophore-based virtual screening

Based on the pharmacophore established above, Specs and NCI database was prepared and filtered primarily. Depending on the critical features of Hsp90-Cdc37, the standard charge of each compound in the database was calculated at neutral condition (pH = 7.4). All compounds were prepared using ligand prepare protocol in Discovery Studio 3.0. However,

considering the complexity of the pharmacophore model and harsh screening criteria for eligible ligands, one feature could be omitted in the ligand-pharmacophore mapping procedure. During this process, shape constraints were also applied to maintain the proper conformation of the ligands. Only 1532 compounds in the database, which mapped to the pharmacophore model, were retained for further docking filtration. Libdock, Ligandfit and CDDOCKER were sequentially applied to evaluate the binding capacity of the filtered compounds. Finally, we purchased 31 compounds that satisfied all the demands mentioned above. The whole screening process is shown in Fig. 3.

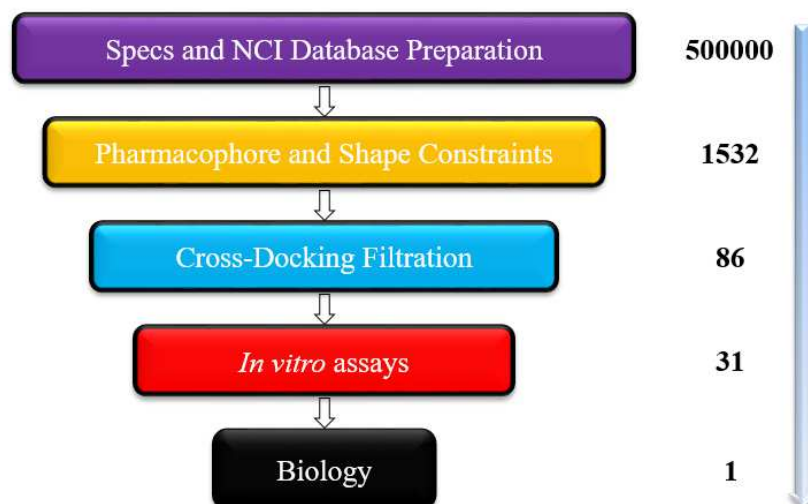


Figure 3. Multistep virtual screening and biology validation strategy for the discovery of modulators targeting Hsp90-Cdc37 PPI.

3.3 *In vitro* validation of virtual hits

The virtual screened hit compounds were subsequently determined by a series of *in vitro* biological assays including homogeneous time-resolved fluorescence (HTRF) assay, ATPase inhibition assay, fluorescence polarization (FP) assay and direct binding assay (biolayer interferometry, BLI). HTRF is a sensitive method to determine the effect of protein-protein interaction based on a time-resolved fluorescence resonance energy transfer

(TR-FRET) mechanism. When Hsp90 bound to Cdc37, the conjugated donor and acceptor came into close proximity to exhibit high emission spectrum. Once the interaction between two proteins is disrupted or affected by inhibitors, the emission spectrum will reduce accordingly [31]. As shown in Table 1, HTRF assay was utilized to verify the potency of all compounds to disrupt Hsp90-Cdc37 PPI *in vitro*. The detailed chemical structures are shown in Fig.4. As shown in the results in Table 1, compound **VS-2**, **VS-8**, **VS-22** and **VS-25** exert more than 30% inhibition at the concentration of 100 μ M. Considering all hits might directly bind to Hsp90 N-terminal, an FP competitive assay was performed to determine whether these compounds could occupy the ATP binding site of Hsp90. The detailed method was reported previously [32]. Based on FITC labeled Geldanamycin, the first identified Hsp90 ATPase inhibitor, all the compounds showed no binding at 100 μ M ligand concentration which demonstrated an obvious difference between these compounds and classic Hsp90 N-terminal inhibitors. To examine the effect of ATPase inhibition, an assay of the Discover RX ADP HunterTM Plus Assay Kit was performed. The final data showed that compound **VS-2**, **VS-8** and **VS-25** exhibited no influence on Hsp90 ATPase even when the concentration raised up to 100 μ M. However, **VS-22** revealed a weak inhibition as 45.67% which might be a result of resemble structure to purine analogues. Among all the assays, celastrol was used as a positive control to show 79.34% inhibition in HTRF assay while little inhibition effect in ATPase and FP assay at 100 μ M was observed, which is consistent with literature reports [20]. **17-DMAG**, a classic Hsp90 ATPase inhibitor, exerted no Hsp90-Cdc37 PPI disruption ability but high inhibitory effect in ATPase and FP assay (shown in Table 2).

Subsequently, biolayer interferometry (BLI) assay, which is identified as one of the most common ways to determine the direct binding affinity of ligand-protein interactions

[33], was applied to examine the direct binding capacity of these four compounds. A dose-dependent binding manner was observed according to the association and dissociation curves. K_D values were calculated by the equation: $K_D = K_{off}/K_{on}$. Finally, **VS-8** obtained a measured K_D value of 80 μ M. Compound **VS-2** and **VS-25** exhibited no binding while **VS-22** exerted a quite feeble binding ability ($> 100 \mu$ M). The data of the *in vitro* assays we obtained showed that **VS-8** could bind to Hsp90 with a moderate binding ability, exhibiting an entirely different binding mechanism with Hsp90 ATPase inhibitors. **VS-8** exerted no effect on Hsp90 ATPase while disrupted Hsp90-Cdc37 PPI with micromolar inhibitory activity in HTRF assay through a direct binding manner. Although **VS-8** gave its potential to disrupt Hsp90-Cdc37 PPI, the potency of **VS-8** is feeble which needs a series of derivatives for further investigations.

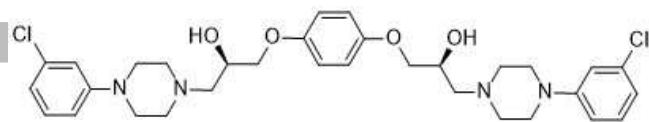
Table 1 100 μ M inhibition and binding constants (K_D) of 4 compounds ^c

Compound No.	HTRF inhibition (100 μ M)	ATPase inhibition (100 μ M)	FP inhibition (100 μ M)	K_D (BLI)
VS-2 (AP-263/41670332)	47.64%	< 10%	N/A ^a	N/A
VS-8 (AN-329/40718894)	59.33%	< 10%	N/A ^a	80.4 μ M
VS-22 (AP-906/41637264)	36.59%	45.67%	N/A ^a	> 100 μ M
VS-25 (AM-900/14781022)	30.67%	< 10%	N/A ^a	N/A
Celastrol (10 μ M)	79.34%	12.31%	N/A ^a	ND ^b
17-DMAG (10 μ M)	N/A ^a	96.45%	99.82%	ND ^b

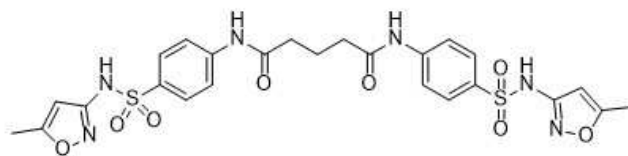
^a No activity

^b Not determined

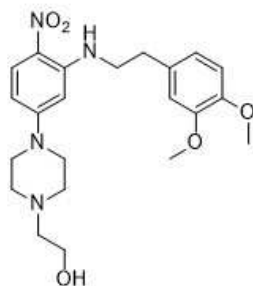
^c all values are the mean of three independent experiments.



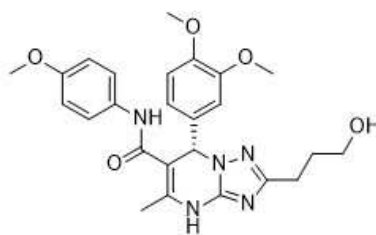
VS-2



VS-8



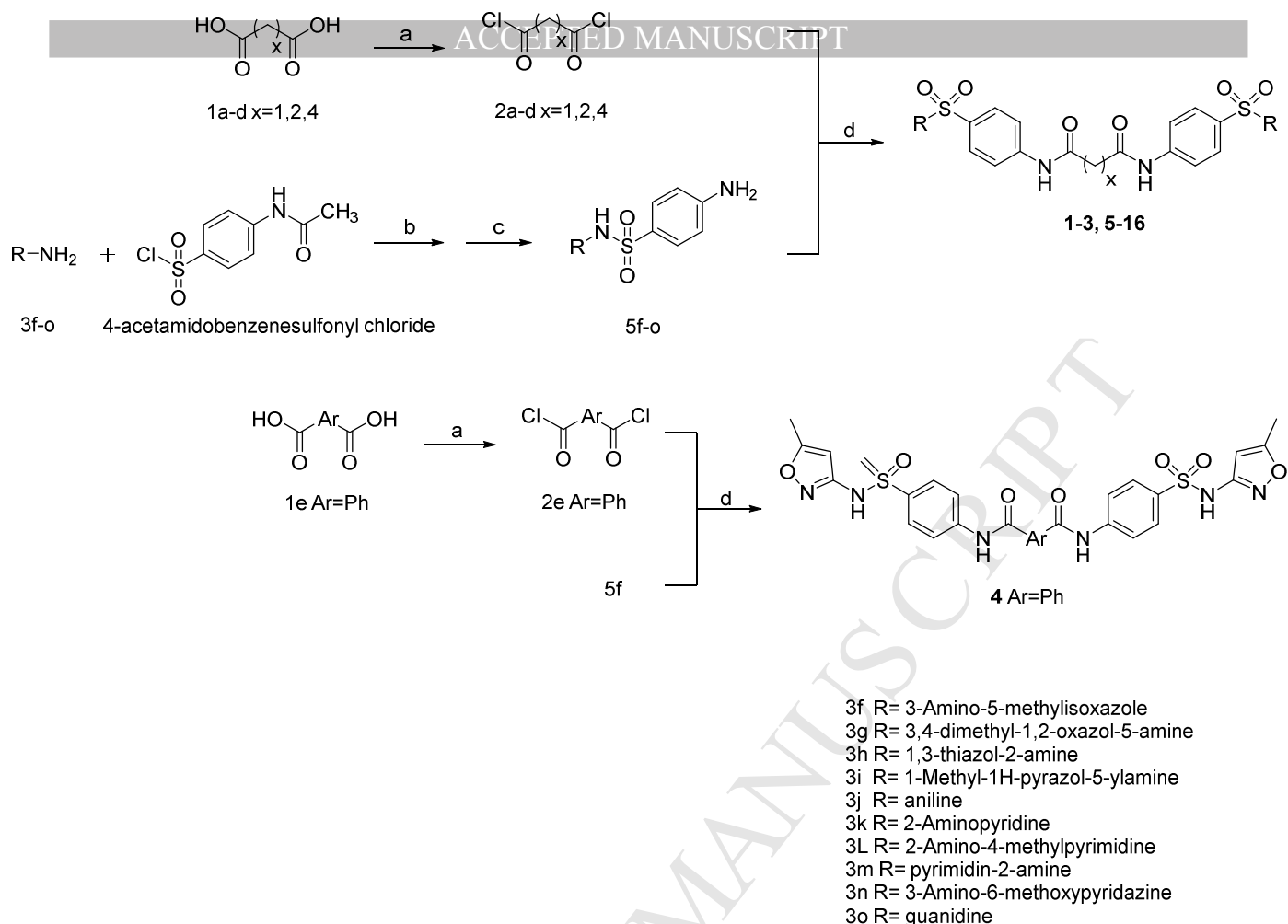
VS-22



VS-25

Figure 4. Chemical structures of four virtual screened hits, VS-2, VS-8, VS-22, VS-25.

3.4 Potential binding model analysis and Structure activity relationship study of VS-8



Scheme 1: Reagents and conditions: a) $SOCl_2$, reflux; b) THF, pyridine, rt; c) 20% NaOH solution, reflux; d) THF or 1,4-dioxane, pyridine, rt.

To confirm the potency of VS-8, a series of derivatives were designed and synthesized. VS-8 is a symmetrical structure containing a central benzamide with three alkyl carbons as a linker to perform as two equal aromatic systems by connecting a sulfonamide. In order to have a better understanding of VS-8 binding mode for further compounds design, we modeled VS-8 into Hsp90-Cdc37 binding site using the crystal structure (PDB: 1US7). As shown in Fig 5A and 5B, VS-8 could bind to Hsp90 by occupying both P1, P2 and P3 sub-pockets to exert potential disruption ability of Hsp90-Cdc37 PPI. One of the methyl oxazole side-chain occupied P1 (including Leu93, Ala97, Phe124 and Tyr125) and the other formed hydrogen bond with Gln119 in Hsp90 to occupy P3. The central linker chain with

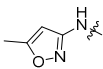
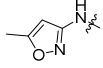
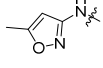
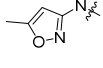
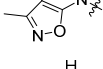
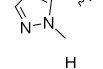
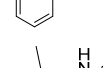
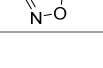
five carbon atoms bound to P2 and formed interactions with Asn37 and Gln119 through its amides. Based on this point of view, the major concerns for optimization of **VS-8** might include linker chain variations to obtain a better ligand efficiency in P2 and different aromatic substitutions to form extra possible interactions with Hsp90, especially in P3 which exert fewer interactions.

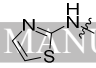
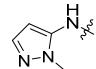
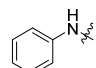
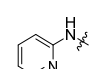
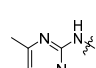
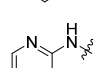
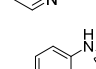
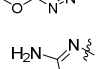
Subsequently, we first explored the main linker on the original structure by altering the amount of middle alkyl carbons or directly replacing it with phenyl ring while the original sulfonamide substitution was maintained. Different lengths of alkyl carbons (from one to four) were utilized to obtain main linker variation derivatives **1-3** and phenyl ring substituted compound **4** according to a two-step synthetic route, shown in **Scheme 1**. As shown in Table 2, besides compound **4**, the derivatives (compounds **1-3**) of main linker variations slightly affected the inhibition in HTRF assay under the compound concentration of 100 μ M which indicated that phenyl ring was not favored in central linker modifications. Among them, compound **1** and **2** exhibited the optimal inhibition of 66% and 70%, respectively. Based on this result, the central linker length of one to two alkyl carbons might be the most ideal to exert optimal occupation of P2. Further modifications of different substitutions of sulfonamide were designed to rigidify the one/two carbon linker and explored the significance of different heterocyclic ring of the negative charge/H-bond acceptors to form more interactions in P1 and P3. Using the scaffold of several penta/hexa-heterocycles as the sidechain amide modifications, compounds **5-16** were obtained as second series of symmetrical compounds. The preparation pathway of compounds **5-16** from 5f-5o with 2a-2d was shown in **Scheme 1**. Unfortunately, the majority of these compounds **5-16** exhibited declined or lost activity (less than 50% inhibition under 100 μ M), except compound **10** with N-methylpyrazole substitution and the central linker of two alkyl carbons

exhibited slightly improved activity. Using the same model as **VS-8**, we modeled compound **10** to the same binding site of Hsp90-Cdc37 PPI. As shown in Fig. 5C and 5D, compound **10** exerted similar binding mode as **VS-8**. As we expected, the central linker shrinkage made this chain more unfolded which might result in a higher ligand efficiency in occupation of P2, leading to the formation of significant interactions between amides and Arg32, Glu33 as well as Ser36. N-methylpyrazole substitution in P1 formed similar interactions (interacted with Ala97, Val122 and Tyr125) with **VS-8**. Additionally, N-methylpyrazole substitution in P3 could form more interactions with multiple residues including Ser198, Glu199 and Phe200 which might result in a better activity.

To further evaluating the detailed inhibitory activity and binding capacity between compound **10** and **VS-8**, we calculated the IC_{50} values using HTRF assay and determined the binding constants using biolayer interferometry assay. As shown in Fig. 6, compound **10** exhibited more promising inhibitory effect ($IC_{50} = 27.40 \mu\text{M}$) compared to **VS-8** ($IC_{50} = 76.85 \mu\text{M}$).

Table 2.SAR exploration of central linker and sidechain substitution.^a

Com.	x or Ar	R	Inhibition % (100 μM)
1	-CH ₂ -		65.6
2	-CH ₂ CH ₂ -		69.8
3	-CH ₂ CH ₂ CH ₂ CH ₂ -		20.7
4	-Ph-		NA
5	-CH ₂ -		< 10%
6	-CH ₂ -		50.9
7	-CH ₂ -		30.4
8	-CH ₂ CH ₂ -		48.7

9	-CH ₂ CH ₂ -		< 10
10	-CH ₂ CH ₂ -		79.4
11	-CH ₂ CH ₂ -		49.6
12	-CH ₂ CH ₂ -		< 10
13	-CH ₂ CH ₂ -		< 10
14	-CH ₂ CH ₂ -		< 10
15	-CH ₂ CH ₂ -		< 10
16	-CH ₂ CH ₂ -		< 10
VS-8			59.3
Celastrol			92.3

^a all values are the mean of three independent experiments.

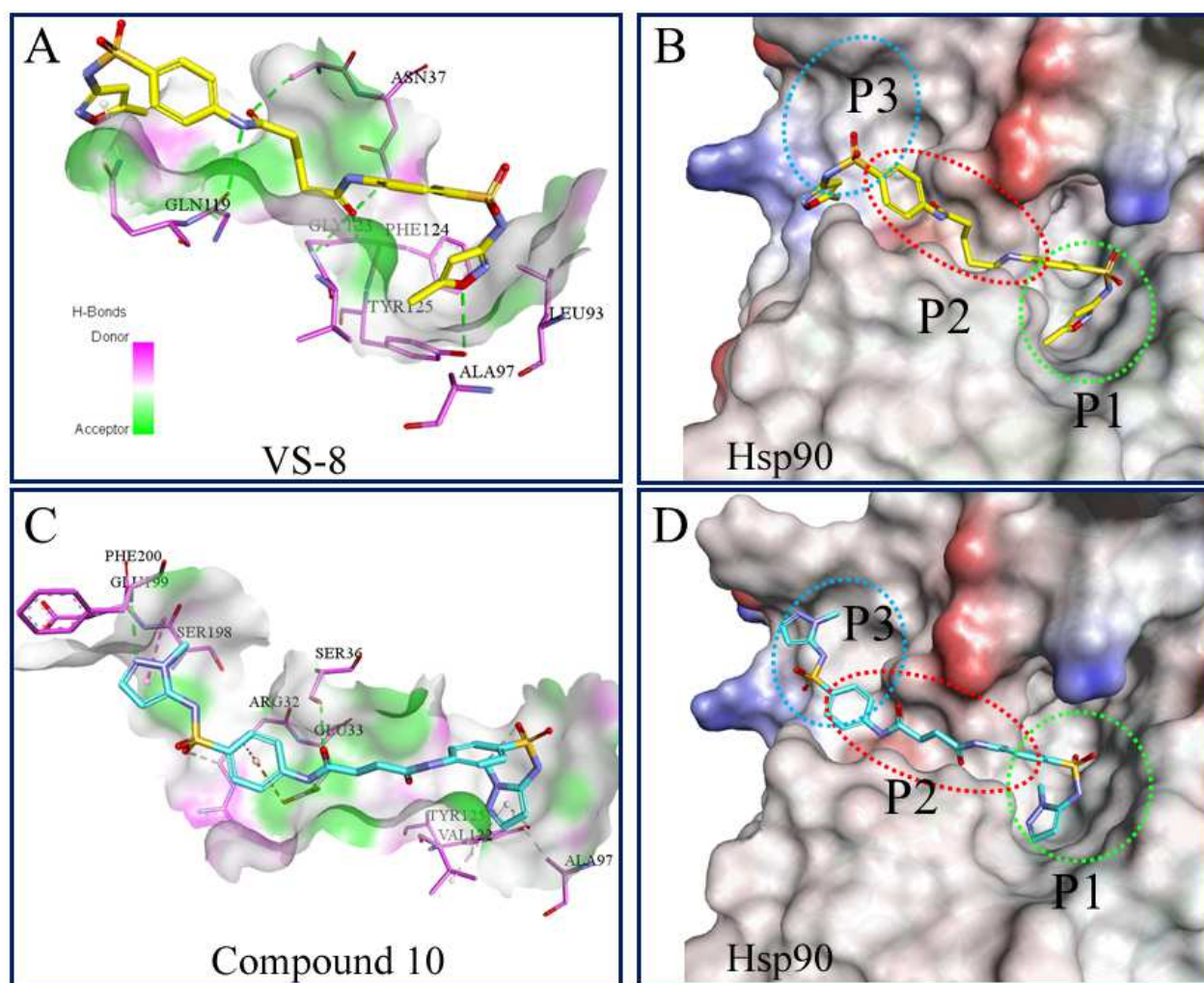


Figure 5. Potential binding models of **VS-8** and compound **10**. The surface of Hsp90 was colored. (A,C)

Interaction modes of the **VS-8** and compound **10** respectively. Compound **10** formed extra multiple interactions with Hsp90 compared to **VS-8**. (B,D) Binding surface depiction of the **VS-8** and compound **10**. Both two compounds occupied the P1, P2 and P3 sub-pockets. Compound **10** performed better conformational occupation in P1 and P2 with the central linker shrinkage and N-methylpyrazole substitution of the side-chain in **VS-8**.

3.5 Compound 10 disrupts Hsp90-Cdc37 PPI *in vitro*, exhibits anti-proliferative capacity and down-regulates the expression of client proteins

To confirm the PPI disruption ability of compound **10**, we utilized a GST-pull down assay kit for further validation. Detailed experiment procedure was described in the methods and materials. After all the eluted liquids were analyzed by SDS-PAGE and western-blot with anti-tag antibody (anti-GST and anti-His). Three concentrations of compound **10** were set from 1 μM to 20 μM and two concentrations of celastrol were set as 1 μM and 20 μM which including two same concentrations of these two compounds. As shown in Fig. 6C, compound **10** exhibited little inhibition ability at the concentration of 1 μM and 5 μM , but almost completely abrogated the interaction of Hsp90 with Cdc37 at the 20 μM concentration. In addition, celastrol could also completely disrupted the interaction between Hsp90-Cdc37 at 20 μM concentration. All these data demonstrated that compound **10** could disrupt the interaction between Hsp90-Cdc37 *in vitro* through a concentration-dependent manner and exhibit similar disruption ability compared with celastrol.

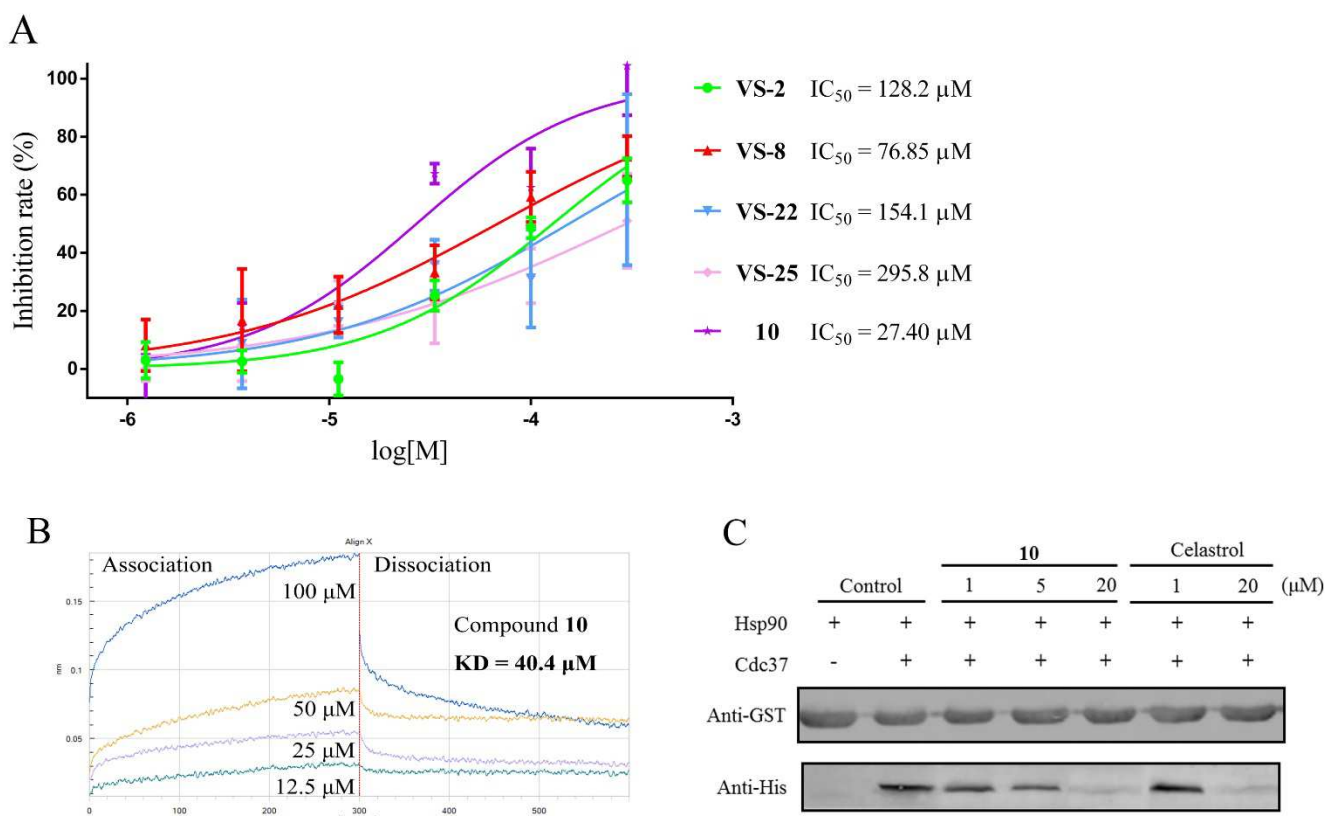


Figure 6. (A) Dose-dependent inhibition of compound **VS-2**, **VS-8**, **VS-22**, **VS-25** and compound **10** in the HTRF assay. (B) Biolayer interferometry sensorgrams of the binding of multiple concentrations of **VS-8** to Hsp90. (C) compound **10** and **VS-8** disrupt Hsp90-Cdc37 *in vitro* through a concentration-dependent manner by GST-pull down assay.

It has been reported that Hsp90 and Cdc37 revealed high relevance with the occurrence and development of cancer [14, 34]. The anti-proliferative capacities of 5 compounds and celastrol were determined by MTT assay against the human breast cancer MCF-7 and SKBR3 cell lines as well as non-small cell lung cancer cell line A549. Cells were treated with various concentration (ranging from 200 μM to 0.823 μM with three times dilution) of compounds for 72 h. The cell viability was assessed by mitochondrial dehydrogenase activity. As shown in Table 3, among all the compounds, compound **10** exhibited the optimal anti-proliferative activity with IC_{50} s of 26 μM , 15 μM and 38 μM against MCF7, SKBR3 and A549, respectively, which indicated a high correlation with previously described *in vitro*

activity. Celastrol exhibited strong anti-proliferative activity with more than 95% inhibition at 10 μ M against all three tested cell lines which was correlated with previous report [35]. Because compound **10** exhibited the potential disruption ability of Hsp90-Cdc37 interaction, we next determined whether compound **10** could exhibit inhibition potential on Hsp90 function and affect the expression levels of its client proteins in breast cancer cell (SKBR3). After treatment of compound **10** and celastrol with various concentrations, we determined the expression levels of two well-known client proteins of Hsp90-Cdc37, Akt and Cdk4 [36, 37]. As shown in Fig. 7, both compound **10** and celastrol decreased the protein levels of Akt and Cdk4 in a concentration-dependent manner. A 24-hour treatment of SKBR3 cells with 10 μ M compound **10** and 1 μ M celastrol moderately decreased Akt and Cdk4, but 50 μ M compound **10** and 10 μ M celastrol could separately down-regulate Akt and Cdk4 obviously. Meanwhile, both compound **10** and celastrol exhibited no effect on the expression level of Hsp90. These data indicated that compound **10** could induce degradation of client proteins of Hsp90-Cdc37 PPI. These results demonstrated that, as potential Hsp90-Cdc37 PPI modulators, compound **10** exhibited micromole binding capacity and anti-proliferative activity which could be recognized as a start point to study Hsp90-Cdc37 PPI and further structural modification might provide insights into modulators development with high affinity.

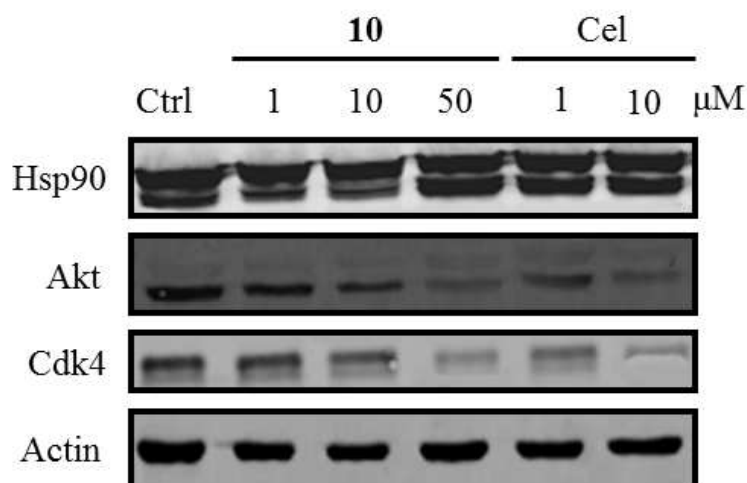


Figure 7. Effects of compound **10** and celastrol on client proteins degradation. Both compound **10** and celastrol induces decreases of Hsp90 client proteins (Akt and Cdk4) through a concentration -dependent manner by Western blot. Meanwhile, compound **10** and celastrol have no effect on the expression level of Hsp90.

Table 3. IC₅₀ values of selected compounds *in vitro* antitumor activity.

Cpd	antiproliferative activities IC ₅₀ (μM) ^a		
	MCF-7	SKBR-3	A549
VS-2	89.18 ± 5.98	> 100	> 100
VS-8	66.91 ± 4.21	59.44 ± 2.99	75.31 ± 6.19
VS-22	> 100	> 100	> 100
VS-25	> 100	84.56 ± 6.13	> 100
10	26.42 ± 2.86	14.67 ± 1.98	38.44 ± 2.17
Celastrol (10 μM)	98.62%	97.62%	95.43%

^a Values shown are the mean ± SD (n=3).

4. Conclusions and Discussion

In recent years, Hsp90-Cdc37 PPI has been recognized as an alternative strategy to achieve Hsp90 inhibition through a non-ATPase dependent way. In addition to classic ATP-competitive Hsp90 inhibitors, disrupting Hsp90-Cdc37 PPI will only affect certain

protein kinases, rather than all the client proteins of Hsp90, which definitely exhibit higher specificity and lower potential toxicity [15]. However, discovery and identification of highly efficient PPI modulators have been regarded as the most challenging tasks in medicinal chemistry. It is common for PPIs to reveal large binding domains and various allosteric sites which make it much more challenging to discover small molecules based on traditional medicinal chemistry methods. Oligopeptides, which are directly derived from the PPI binding interface, could be served as ideal templates to design small molecules. Based on our previous study [27], we utilized the potential peptides derived from Cdc37 to explore the detailed binding site of Hsp90-Cdc37 for the discovery of small molecules. According to the detailed binding mode, five pharmacophores were generated including three H-bond features, one hydrophobic feature and one ionizable feature. All of these features, taken together, could represent the most potential binding sites of Hsp90-Cdc37. We subsequently used this pharmacophore model and cross-docking filtration to screen the Specs and NCI database which resulted in 31 compounds for purchase and evaluation. The data of the *in vitro* assays showed that **VS-8** could bind to Hsp90 with a moderate binding ability, exhibiting an entirely different binding mechanism with Hsp90 ATPase inhibitors. **VS-8** exerted no effect on Hsp90 ATPase while it disrupted Hsp90-Cdc37 PPI with micromole inhibitory activity in HTRF assay through a direct binding manner. To further confirm the potency of **VS-8**, a series of derivatives were designed and synthesized which resulted in compound **10** with N-methylpyrazole substitution and the central linker of two alkyl carbons. Compound **10** exhibited promising inhibitory effect ($IC_{50} = 27 \mu M$), moderate binding capacity ($K_D = 40 \mu M$) and preferable antiproliferative activity against multiple cancer cell lines compared to **VS-8**. All the data suggest that compound **10** exhibited moderate inhibitory effect on Hsp90-Cdc37 and could be regard as a first evidence of a non-natural compound targeting

Hsp90-Cdc37 PPI. Moreover, there is still a tough way to go for discovery of high affinity small molecules targeting Hsp90-Cdc37.

Acknowledgments

This work was supported by Projects 81573346 and 81502990 of the National Natural Science Foundation of China; BK20150691 of the Natural Science Foundation of Jiangsu Province; 2105ZD009 of the Key Program of China Pharmaceutical University; 2103ZX09402102-001-005 of the National Major Science and Technology Project of China (Innovation and Development of New Drugs); and a Project Funded by the Priority Academic Program Development of Jiangsu Higher Education Institution.

References

1. Chiosis G, Dickey CA, Johnson JL. A global view of Hsp90 functions, *Nat Struct Mol Biol.* 20.(2013),1-4.
2. Mahalingam D, Swords R, Carew JS, Nawrocki ST, Bhalla K, Giles FJ. Targeting HSP90 for cancer therapy, *Br J Cancer.* 100.(2009),1523-1529.
3. Scaltriti M, Dawood S, Cortes J. Molecular pathways: targeting hsp90--who benefits and who does not, *Clin Cancer Res.* 18.(2012),4508-4513.
4. Bhat R, Tummalapalli SR, Rotella DP. Progress in the discovery and development of heat shock protein 90 (Hsp90) inhibitors, *J Med Chem.* 57.(2014),8718-8728.
5. Garcia-Carbonero R, Carnero A, Paz-Ares L. Inhibition of HSP90 molecular chaperones: moving into the clinic, *The Lancet Oncology.* 14.(2013),e358-e369.
6. Jhaveri K, Taldone T, Modi S, Chiosis G. Advances in the clinical development of heat shock protein 90 (Hsp90) inhibitors in cancers, *Biochim Biophys Acta.* 1823.(2012),742-755.
7. Rajan A, Kelly RJ, Trepel JB, Kim YS, Alarcon SV, Kummar S, Gutierrez M, Crandon S, Zein WM, Jain L *et al.* A phase I study of PF-04929113 (SNX-5422), an orally bioavailable heat shock protein 90 inhibitor, in patients with refractory solid tumor malignancies and lymphomas, *Clin Cancer Res.* 17.(2011),6831-6839.
8. Whitesell L, Bagatell R, Falsey R. The stress response: implications for the clinical development of hsp90 inhibitors, *Curr Cancer Drug Targets.* 3.(2003),349-358.
9. Prodromou C. The 'active life' of Hsp90 complexes, *Biochim Biophys Acta.* 1823.(2012),614-623.
10. Calderwood SK. Molecular cochaperones: tumor growth and cancer treatment, *Scientifica (Cairo).* 2013.(2013),217513.
11. Retzlaff M, Hagn F, Mitschke L, Hessling M, Gugel F, Kessler H, Richter K, Buchner J. Asymmetric activation of the hsp90 dimer by its cochaperone aha1, *Mol Cell.* 37.(2010),344-354.
12. Kang BH, Altieri DC. Compartmentalized cancer drug discovery targeting mitochondrial Hsp90 chaperones, *Oncogene.* 28.(2009),3681-3688.
13. Pearl LH. Hsp90 and Cdc37 -- a chaperone cancer conspiracy, *Curr Opin Genet Dev.* 15.(2005),55-61.

14. Vaughan CK, Mollapour M, Smith JR, Truman A, Hu B, Good VM, Panaretou B, Neckers L, Clarke PA, Workman P *et al.* Hsp90-dependent activation of protein kinases is regulated by chaperone-targeted dephosphorylation of Cdc37. *Mol Cell.* 31.(2008),886-895.
15. Workman JRSaP. Targeting CDC37 : An alternative, kinase-directed strategy for disruption of oncogenic chaperoning. *Cell Cycle.* 8.(2009),362-372.
16. Olesen SH, Ingles DJ, Zhu JY, Martin MP, Betzi S, Georg GI, Tash JS, Schonbrunn E. Stability of the human Hsp90-p50Cdc37 chaperone complex against nucleotides and Hsp90 inhibitors, and the influence of phosphorylation by casein kinase 2. *Molecules.* 20.(2015),1643-1660.
17. Roe SM1 AM, Meyer P, Vaughan CK, Panaretou B, Piper PW, Prodromou C, Pearl LH. The Mechanism of Hsp90 regulation by the protein kinase-specific cochaperone p50(cdc37). *Cell.*(2004).
18. Sreeramulu S, Jonker HR, Langer T, Richter C, Lancaster CR, Schwalbe H. The human Cdc37.Hsp90 complex studied by heteronuclear NMR spectroscopy. *J Biol Chem.* 284.(2009),3885-3896.
19. Roe SM, Ali MM, Meyer P, Vaughan CK, Panaretou B, Piper PW, Prodromou C, Pearl LH. The Mechanism of Hsp90 regulation by the protein kinase-specific cochaperone p50(cdc37). *Cell.* 116.(2004),87-98.
20. Zhang T, Hamza A, Cao X, Wang B, Yu S, Zhan CG, Sun D. A novel Hsp90 inhibitor to disrupt Hsp90/Cdc37 complex against pancreatic cancer cells. *Mol Cancer Ther.* 7.(2008),162-170.
21. Zhang T, Li Y, Yu Y, Zou P, Jiang Y, Sun D. Characterization of celastrol to inhibit hsp90 and cdc37 interaction. *J Biol Chem.* 284.(2009),35381-35389.
22. Grover A, Shandilya A, Agrawal V, Pratik P, Bhasme D, Bisaria VS, Sundar D. Hsp90/Cdc37 chaperone/co-chaperone complex, a novel junction anticancer target elucidated by the mode of action of herbal drug Withaferin A. *BMC Bioinformatics.* 12 Suppl 1.(2011),S30.
23. Huang W, Ye M, Zhang L-r, Wu Q-d, Zhang M, Xu J-h, Zheng W. FW-04-806 inhibits proliferation and induces apoptosis in human breast cancer cells by binding to N-terminus of Hsp90 and disrupting Hsp90-Cdc37 complex formation. *Mol Cancer.* 13.(2014),150.
24. Zhao M, Ma J, Zhu HY, Zhang XH, Du ZY, Xu YJ, Yu XD. Apigenin inhibits proliferation and induces apoptosis in human multiple myeloma cells through targeting the trinity of CK2, Cdc37 and Hsp90. *Mol Cancer.* 10.(2011),104.
25. Li Y, Karagoz GE, Seo YH, Zhang T, Jiang Y, Yu Y, Duarte AM, Schwartz SJ, Boelens R, Carroll K *et al.* Sulforaphane inhibits pancreatic cancer through disrupting Hsp90-p50(Cdc37) complex and direct interactions with amino acids residues of Hsp90. *J Nutr Biochem.* 23.(2012),1617-1626.
26. Milroy LG, Grossmann TN, Hennig S, Brunsveld L, Ottmann C. Modulators of protein-protein interactions. *Chem Rev.* 114.(2014),4695-4748.
27. Wang L, Li L, Fu WT, Jiang ZY, You QD, Xu XL. Optimization and bioevaluation of Cdc37-derived peptides: An insight into Hsp90-Cdc37 protein-protein interaction modulators. *Bioorg Med Chem.*(2016).
28. Sun HP, Jia JM, Jiang F, Xu XL, Liu F, Guo XK, Cherfaoui B, Huang HZ, Pan Y, You QD. Identification and optimization of novel Hsp90 inhibitors with tetrahydropyrido[4,3-d]pyrimidines core through shape-based screening. *Eur J Med Chem.* 79.(2014),399-412.
29. Wang L, Bao Q-C, Xu X-L, Jiang F, Gu K, Jiang Z-Y, Zhang X-J, Guo X-K, You Q-D, Sun H-P. Discovery and identification of Cdc37-derived peptides targeting the Hsp90-Cdc37 protein-protein interaction. *RSC Adv.* 5.(2015),96138-96145.
30. Leach AR, Gillet VJ, Lewis RA, Taylor R. Three-dimensional pharmacophore methods in drug discovery. *J Med Chem.* 53.(2010),539-558.
31. Jia Y. Current status of HTRF((R)) technology in kinase assays. *Expert Opin Drug Discov.* 3.(2008),1461-1474.
32. Kim J, Felts S, Llauger L, He H, Huezos H, Rosen N, Chiosis G. Development of a fluorescence polarization assay for the molecular chaperone Hsp90. *J Biomol Screen.* 9.(2004),375-381.
33. Geschwindner S, Ulander J, Johansson P. Ligand Binding Thermodynamics in Drug Discovery: Still a Hot Tip?. *J Med Chem.* 58.(2015),6321-6335.
34. Xu W, Neckers L. The double edge of the HSP90-CDC37 chaperone machinery: opposing determinants of kinase stability and activity. *Future Oncol.* 8.(2012),939-942.

35. Kannaiyan R, Shanmugam MK, Sethi G. Molecular targets of celastrol derived from Thunder of God Vine: potential role in the treatment of inflammatory disorders and cancer, *Cancer Lett.* 303.(2011),9-20.
36. Sato S, Fujita N, Tsuruo T. Modulation of Akt kinase activity by binding to Hsp90, *P Natl Acad Sci USA.* 97.(2000),10832-10837.
37. Stepanova L, Leng XH, Parker SB, Harper JW. Mammalian p50(Cdc37) is a protein kinase-targeting subunit of Hsp90 that binds and stabilizes Cdk4, *Genes & Development.* 10.(1996),1491-1502.

ACCEPTED MANUSCRIPT

Highlights

1. A multiple workflow including structure-based virtual screening, derivatives synthesis and biological tests was established.
2. **VS-8** exhibited potential ability to disrupt Hsp90-Cdc37 interaction *in vitro* at micromole level.
3. Synthesis of **VS-8** derivatives was performed based on binding mode.
4. Compound **10** exhibited better Hsp90-Cdc37 inhibition ability and revealed anti-proliferative activity by down-regulating client proteins.